Weak Interaction, Marginal Miscibility, and Ring-Band Spherulites in Blends of Poly(vinylidene fluoride) with Polyesters

Shu Hsien Li, E. M. Woo

Department of Chemical Engineering, National Cheng Kung University, Tainan 701-01, Taiwan

Received 23 March 2007; accepted 21 June 2007
DOI 10.1002/app.27111
Published online 25 September 2007 in Wiley InterScience (www.interscience.wiley.com).

ABSTRACT: Fourier transform infrared (FTIR) spectroscopy, optical microscopy (OM), and differential scanning calorimetry (DSC) techniques were used to probe phase behavior and interactions in blends of poly(vinylidene fluoride) (PVDF) and polyesters [poly(trimethylene adipate) (PTA) and poly(pentamethylene adipate) (PPA)] of relatively low crystallizability. DSC thermal analysis and OM characterization proved that PVDF was miscible with PTA and PPA with a low lower critical solution temperature. Small negative values of the interaction parameters ($\chi_{12} = -0.13$ for a PVDF/PPA blend) were obtained with the melting-point depression method. FTIR spectroscopy results revealed that interactions between $-CF_2$ of PVDF and the $-C=O$ group of the polyester were weak, in agreement with the thermal analysis results. An increase in the coarseness and/or ring-band spacing further provided supportive evidence that miscibility did exist between the polyester and PVDF constituents in the blends. Pattern changes in ring-band spherulites of the miscible blends further substantiated the favorable, though weak, interactions between the PVDF and polyester constituents. © 2007 Wiley Periodicals, Inc. J Appl Polym Sci 107: 766–777, 2008

Key words: miscibility; polyesters; PVDF; ring bands

INTRODUCTION

There are very few claimed cases of miscibility in blends of poly(vinylidene fluoride) (PVDF) with polyesters. Blends of PVDF with aryl polyesters are mostly immiscible. Furthermore, most blends of PVDF with aliphatic polyesters are also immiscible. PVDF is immiscible with polyesters such as poly(ethylene succinate) and poly(ethylene adipate) (PEA). A PVDF/poly(ε-caprolactone) (PCL) blend is also classified as being immiscible.[1,2] In addition, poly(L-lactic acid) is immiscible with PVDF. Surprisingly, although the fluoro structure in PVDF may be expected to exhibit H-bonding interactions with the carbonyl groups in polyesters (either aryl or aliphatic ones), it appears that PVDF is immiscible with most carbonyl-containing polyesters. Only a few miscible PVDF/polyester blends can be cited. Miscibility in blends of PVDF and poly(1,4-butylene adipate) (PBA),[3,4] PVDF and poly(1,4-butylene succinate) (PBSu),[5,6] and PVDF and poly(ethylene terephthalate) (PET)[7] has been reported. Note that the evidence for miscibility in those cited reports, however, is not unambiguously positive for blends involving PVDF and polyesters. Usually, the glass-transition temperature (T_g)–composition behavior in PVDF/polyester blends cannot be shown positively as evidence for phase homogeneity. T_g–composition relationships for those claimed miscible blend systems can be established only in the PVDF-rich range, whereas the polyester-rich compositions of the blends usually yield an ambiguous T_g transition that is usually masked by either the polyester's crystallinity or complex phase behavior. Poly(β-hydroxy butyrate) (PHB) has been claimed to be miscible with PVDF.[8–10] However, in those claimed miscible blends of PVDF and PHB, usually T_g–composition behavior has not been shown, and only substitutive methods of characterization have been discussed. In other words, miscibility in those claims may not be so clearly persuasive.

In comparison, PVDF is more evidently miscible with other carbonyl-containing polymers, such as some polyacrylates. Miscibility has been reported in PVDF/poly(methyl methacrylate) (PMMA), PVDF/poly(methyl acrylate), PVDF/poly(ethyl acrylate), and PVDF/poly(ethyl methacrylate).[11–14] These carbonyl-containing acrylic polymers, in contrast to aryl or aliphatic polyesters, are mostly amorphous in nature. In these miscible blends, T_g–composition behavior is much more clearly demonstrated to show unambiguous miscibility. Other known miscible blends are demonstrated in cases such as PVDF/poly(vinyl methyl ketone) (PVMK).[1] PVDF is also

Correspondence to: E. M. Woo (emwoo@mail.ncku.edu.tw).

Contract grant sponsor: National Science Council of Taiwan (for three consecutive years); contract grant number: NSC-94 2216 E006 003.

miscible with poly(vinyl acetate) (PVAc).[12,15,16] A rare case of a ternary blend with full miscibility is also demonstrated in PVDF/PVAc/PMMA.[17] The aforementioned miscible blends all show lower critical solution temperature (LCST) behavior, with the phase transforming from miscibility to immiscibility at elevated temperatures. Miscibility in these blends of PVDF with carbonyl-containing polymers is generally attributed to polar interactions between CF_2 and C=O. However, the literature apparently shows that not all C=O-containing polymers are miscible with PVDF. Thus, polar interactions between CF_2 and C=O are not a necessary condition for miscibility in blends of polyesters with PVDF; there must be some other factors exerted by the polyester's chain structure that determine the most suitable environment for polar interactions leading to miscibility.

Thus, it is puzzling that PVDF can be miscible with several amorphous polymers such as PVAc, PMMA, and PVMK that are amorphous and have carbonyls in pendant groups; peculiarly, it is not so readily miscible with most semicrystalline polyesters that have carbonyls in the main chain. A more thorough search may be needed through an understanding of the relationships between polyester structural factors and miscibility between PVDF and polyesters. Most polyesters are semicrystalline; thus, PVDF/polyester blends will be crystalline/crystalline systems. Effects of crystalline domains on amorphous phase behavior may be more complex for crystalline/crystalline blends. It may not be so easy to experimentally deal with the blend phase behavior of the amorphous phases in crystalline/crystalline blends, such as blends of PVDF with semicrystalline polyesters. Two model polyesters with low crystallizability, poly(trimethylene adipate) (PTA) and poly(pentamethylene adipate) (PPA), which are much less crystallizable than most other polyesters, were specifically chosen for investigations of the phase behavior of PVDF blends. Furthermore, ring-band behavior in crystalline regions of the PVDF blends was further probed to substantiate phase behavior in the amorphous regions of the blends.

EXPERIMENTAL

Materials

PVDF was obtained from Scientific Polymer Products, Inc., with a weight-average molecular weight (M_w) of 120,000 g/mol, a T_g value of −40°C, and a melting temperature (T_m) of 158.7°C. Two polyesters were chosen for study because they are much less crystallizable on account of the odd number of methylene groups in glycol units. PTA was purchased from Scientific Polymer Products (M_w = 4000 g/mol, T_g = −62.7°C, T_m = 38°C). Commercial PTAs usually have low molecular weights:

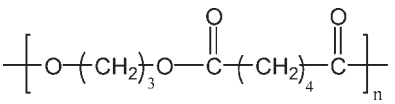

PTA

PPA was not available from commercial sources and was synthesized in house. The synthesis of PPA was performed with a typical procedure for condensation-type polyesters. A flask was charged with a solution of 1,5-pentandiol (3.3 mmol) dissolved in a mixture of 1,1,2,2-tetrachloroethane (10 mL) and 1 mL of pyridine or triethylamine (TEA) under an inert (N_2) atmosphere. Then, adipoyl chloride (3 mmol), dissolved in 1,1,2,2-tetrachloroethane (15 mL), was added dropwise to the mixture at room temperature under N_2. The mixture was subsequently stirred and heated at 75°C for 24 h in a purge of N_2. After the reaction, it was precipitated by the addition of ice methanol and dried *in vacuo*. The molecular weight and polydispersity index (PDI) were determined by GPC (Waters, Milford, MA) with polystyrene as a standard. The characterization data found for PPA were as follows.

M_w = 9000 g/mol. PDI = 1.4. T_g = −58°C. T_m = 33°C. ^{1}H-NMR (400.13 MHz, $CDCl_3$): δ = 4.1 ppm (—COOCH_2—), δ = 2.4 ppm (—COOCH$_2$CH_2—), δ = 1.4 ppm (—COOCH$_2$CH$_2$CH_2—), δ = 1.7 ppm (—COCH_2CH_2—).

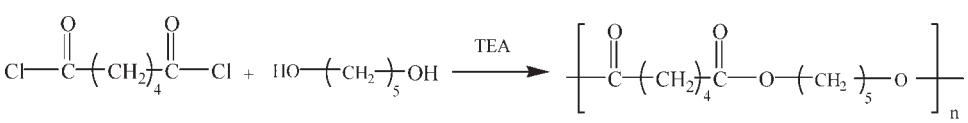

PPA

Sample preparation

Blends of PVDF and PPA (or PTA) were prepared with dimethylformamide as a mutual solvent. The method of melt blending was not attempted as the blends were found to undergo phase separation at high temperatures. Both polymers in the solvent with a concentration of 4 g/100 mL were mixed in the desired proportions and well stirred to a homo-

geneous mixture at 150°C. Sample films were obtained via casting onto glass dishes, on which the solvent in the samples evaporated at 150°C for 24 h, and then the thin films were further dried *in vacuo* (−760 mmHg) at 80°C for 1 week.

Apparatus and procedures

A Nikon Optiphot-2 polarized light microscope (Nikon, Tokyo, Japan) [polarized optical microscopy (POM) or optical microscopy (OM)] with a digital camera (charge-coupled device) was used for characterizing the optical homogeneity and/or crystalline morphology of the blends. A small quantity of the blend samples was transferred between microglass slides, heated, and pressed into thin films (ca. 20 μm) on a heating stage and examined.

T_g transitions of the blend samples were measured with a differential scanning calorimeter (DSC-7, PerkinElmer, Shelton, CT) equipped with an intracooler (to −60°C) and data acquisition/analysis. Additional subambient differential scanning calorimetry (DSC) runs (temperature as low as −100°C) were cooled with a liquid-nitrogen tank and helium-gas purge. Before DSC runs, the temperature and heat of transition of the instrument were calibrated with indium and zinc standards. During thermal annealing or scanning, a continuous nitrogen flow in the DSC sample cell was maintained to ensure minimal sample degradation. For determining the T_g values, a heating rate of 40°C/min was used unless otherwise specified. For erasing the previous thermal history, samples were held at 200°C for 3 min before DSC measurements were started. However, for measurements of T_m, a heating rate of 10°C/min was used instead. For measurements of the equilibrium melting point (T_m^0) of PVDF in PVDF/PPA blends, similar isothermal treatments were imposed on the blend samples. The blend samples were first melted above their respective T_m and then brought (in a DSC cell) to a series of isothermal holding temperatures for crystallization to the full extent. Subsequently, DSC scanning was performed on the isothermally crystallized blend samples to reveal their melting peak(s).

Fourier transform infrared (FTIR) spectroscopy was performed on a Nicolet Magna-560 FTIR instrument. Spectra were obtained at a 4-cm^{-1} resolution, and averages of spectra were obtained from at least 64 scans in the standard wave-number range of 400–4000 cm^{-1}. All samples were solution-cast as thin films directly on KBr pellets for IR characterization. ^{1}H-NMR spectra were taken on a Bruker AMX400 solution NMR instrument (Bruker, Rheinstetten, Germany) operating at 400.13 MHz for proton, and tetramethylsilane was used as the standard.

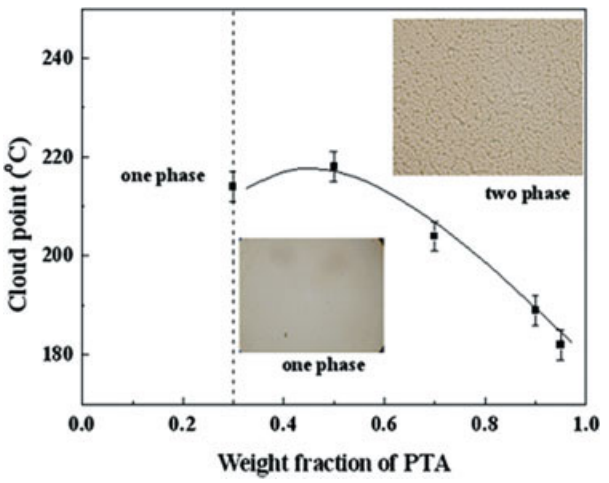

Figure 1 Cloud-point curve and LCST behavior of PVDF/PTA (CH_2/CO = 3.5) blends. [Color figure can be viewed in the online issue, which is available at www.interscience.wiley.com.]

RESULTS AND DISCUSSION

Morphology and thermal evidence

Blends of PVDF with PTA and PPA showed some interestingly common features in phase behavior. As-cast blends of PVDF with these polyesters were clear in amorphous phases (excluding the crystallinity); however, upon heating to higher temperatures, the blends could become cloudy and phase-separated at a certain temperature that varied with the blend compositions. The preliminary observations suggest that an LCST exists in blends of PVDF and PTA (CH_2/CO = 3.5) and PVDF and PPA (CH_2/CO = 4.5). Another blend of PVDF with a polyester of a different structure, PVDF/PBA, was reported earlier by Penning and St. John Manley[3,4] to exhibit similar LCST behavior.

After preliminary screening, focuses of studies were placed then on the PVDF/PTA and PVDF/PPA blends. The PVDF/PTA blend system is discussed first. To further quantify the blend phase transition of the PVDF/PTA blend at specific temperatures, the temperature at which the blends turned to phase separation upon heating was recorded for each of the blend compositions. For convenience, the phase-transition temperature for each blend composition is hereby termed the cloud point for the blend systems with LCST behavior. Figure 1 shows the cloud point and phase boundary for the PVDF/PTA blend of each composition at which the blend turns from a transparent appearance to phase separation upon slow heating (ca. 2°C/min) from T_m of PVDF. The transition temperature (ca. 190–220°C) apparently varies with the composition. However, in contrast to other LCST systems, this blend displays no clear concave shape with a mini-

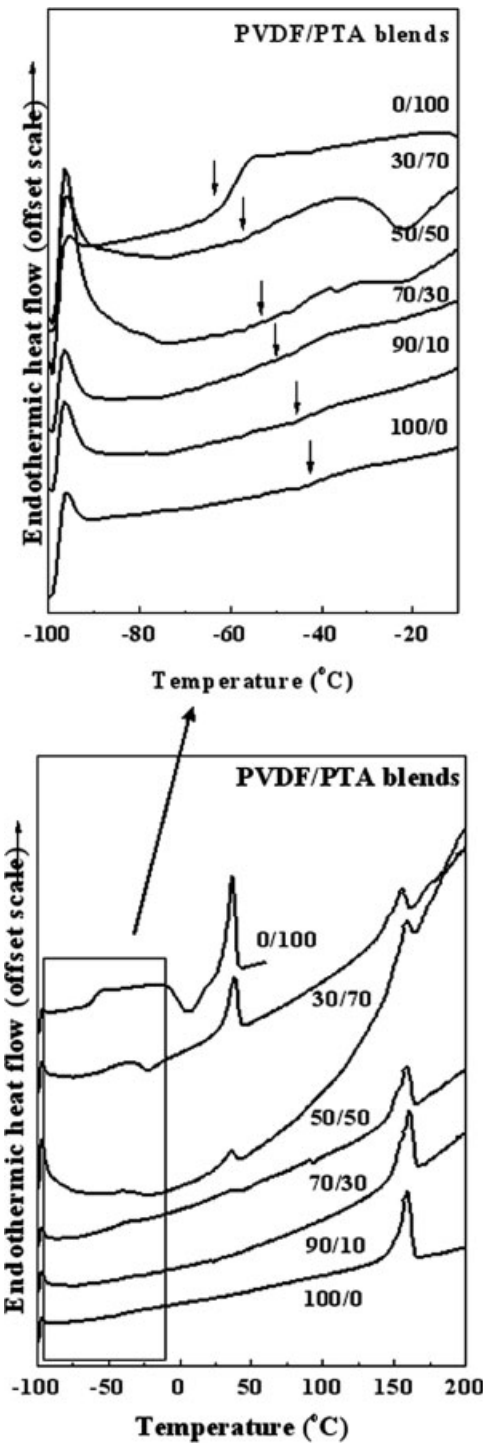

Figure 2 DSC traces for PVDF/PTA blends. The inset shows enlarged T_g regimes.

mum point (LCST). Instead, the temperature of the phase transition in the curve simply monotonously changes with compositions. Note also that the cloud points decrease with the increase in the polyester (PTA) content in the blends, and this indicates that PTA-rich blend compositions are likely associated with fewer interactions between the constituents. The blends of PVDF-rich compositions (PVDF > 70 wt %) are clear and homogeneous with no cloud points detected up to degradation points. DSC thermal analysis was performed on the PVDF/PTA samples to verify a single phase below LCST.

Thermal analysis was performed to reveal the glass-transition behavior in PVDF/PTA blends of various compositions. T_g of the blends was measured on samples held at 200°C for 3 min to erase the previous thermal history and subsequently quenched in DSC at highest possible rates. All discussed results refer to second runs after quenching. Figure 2 shows DSC thermograms for PVDF/PTA blends of various compositions, as indicated in the traces. The DSC results provide evidence of a single T_g for the blends of various compositions, as indicated in the curves. The inset diagram (top) shows enlarged traces on the glass-transition regimes. Note that the T_g signals, extracted from the DSC traces for the PVDF/PTA blends, are much better defined and clearer than other PVDF/polyester blends, such as PVDF/PBA, PVDF/PBSu, and PVDF/PET, that have been reported to be miscible but whose T_g behavior is not clearly defined in the literature.[3–7]

The interactions and T_g–composition relationship for the blends were analyzed for a semiquantitative comparison. The T_g–composition relationship usually provides correlations with interactions or scales of homogeneity in the blends. Figure 3 shows a plot of the T_g data of the blend as a function of the composition. The T_g–composition relationship was test-fitted with a T_g model according to the Gordon–Taylor equation: $T_{g,\text{blend}} = (w_1T_{g1} + w_2kT_{g2})/(w_1 + kw_2)$, with $k = 0.40$. The parameter k is an empirical fitting parameter and w_1 (or 2) is weight fraction of component 1 (or 2). The experimental T_g values with respect to the values predicted by the Couchman–Karasz equation,[18] $\ln(T_{g,\text{blend}}/T_{g2}) = [w_1\Delta C_{p1} \times \ln(T_g/T_{g2})]/(w_1\Delta C_{p1} + w_2\Delta C_{p2})$, are also shown in

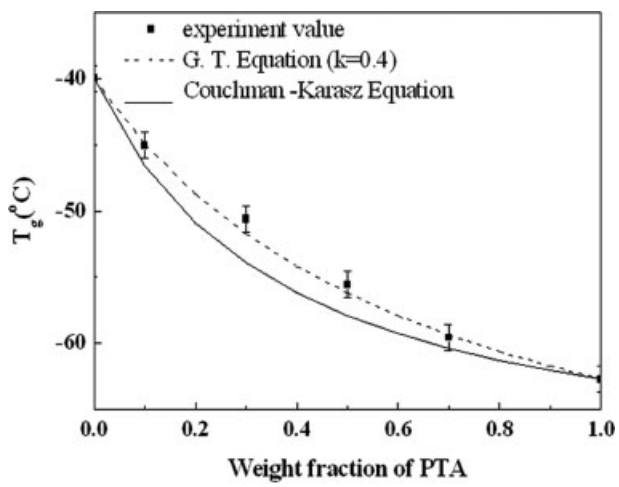

Figure 3 T_g versus the composition for PVDF/PTA blends.

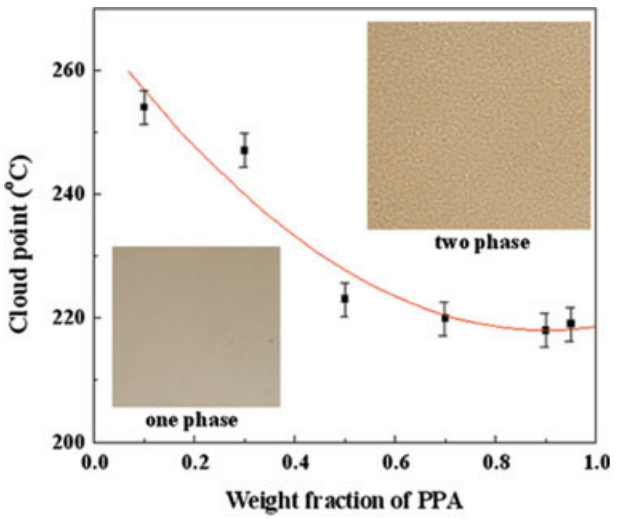

Figure 4 Cloud-point curve and LCST behavior of PVDF/PPA (CH_2/CO = 4.5) blends. [Color figure can be viewed in the online issue, which is available at www.interscience.wiley.com.]

Figure 3. The T_g and molar heat capacities, ΔC_p values are available from the calorimetric measurements of the pure components. Fitting appears quite reasonable within the entire blend composition range. In addition, for other crystalline/crystalline PVDF/polyester blends previously reported,[3–7] such as PVDF/PBA and PVDF/PBSu, DSC traces and T_g signals are usually not well defined, and T_g–composition relationships are either lacking or definable only in a partial composition range.

Furthermore, PPA, with five methylenes between the adipate groups, differs from PTA by two additional methylenes in the repeat unit but is similarly less crystallizable than PTA. Similarly, Figure 4 shows the cloud point, LCST behavior, and phase boundary for the PVDF/PPA blend of each composition at which the blend turns from a transparent appearance to phase separation upon slow heating (ca. 2°C/min) from T_m of PVDF. The transition temperature from miscibility to phase separation (ca. 220–250°C) varies with the composition. The general shape of the cloud-point curve for the PVDF/PPA blend differs significantly from that for the PVDF/PTA blend, but the value of LCST (~ 220°C) is similar to that of the previous blend system (PVDF/PTA). In contrast to other widely reported LCST blends, this blend displays no clear concave shape with a minimum point (LCST). The temperature of the phase transition in the curve monotonously changes with the compositions. Note also that the cloud point decreases with an increase in the polyester (PPA) content in the blends, and this indicates that the PPA-rich blend compositions are likely characterized with less strength of interactions between the constituents in blends. This trend is similar to that for the PVDF/PTA blend system discussed earlier. In comparison with other blends of PVDF and polyesters, the PVDF/PBA blend shows an LCST at 235°C,[3,4] and the PVDF/PBSu blend shows one at 200–240°C.[5,6] The comparison shows that most miscible PVDF/polyester blends possess similar LCST temperatures near 220–250°C, showing

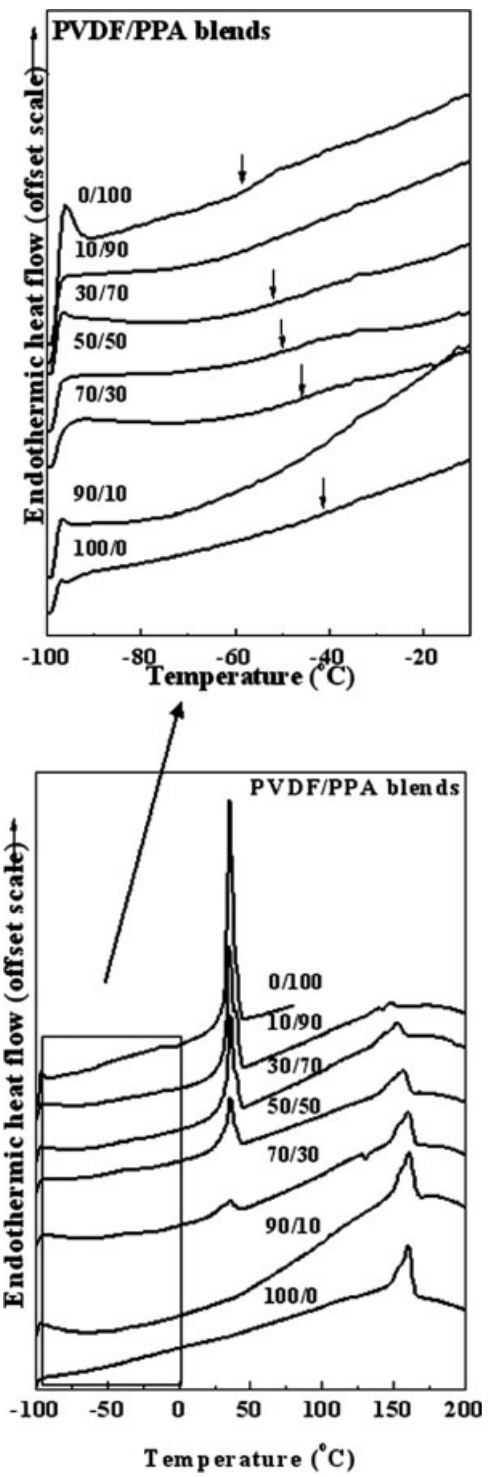

Figure 5 DSC thermograms of PVDF/PPA blends. The inset shows enlarged T_g regimes.

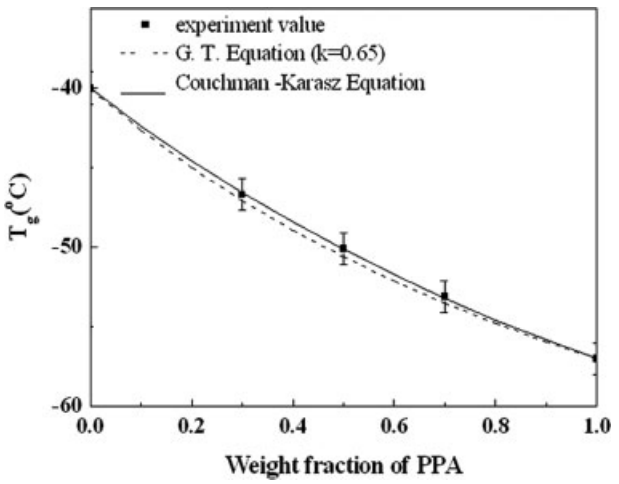

Figure 6 T_g versus the composition for PVDF/PPA blends.

not much variation with respect to the polyester structure.

Thermal analysis was similarly performed on the PVDF/PPA blend samples to verify the single phase below LCST. Figure 5 shows DSC thermograms for PVDF/PPA blends of various compositions, as indicated in traces. The DSC results provide evidence of a single T_g for the blends of various compositions, as indicated in the curves. The inset diagram shows enlarged traces on the glass-transition regimes. The interactions and T_g–composition relationship for the blends were analyzed for a semiquantitative comparison. Figure 6 shows T_g data of the blends plotted as a function of the composition for the PVDF/PPA blends. The T_g–composition relationship was fitted with a T_g model according to the Gordon–Taylor relationship: $T_{g,\text{blend}} = (w_1T_{g1} + w_2kT_{g2})/(w_1 + kw_2)$, with $k = 0.65$. The experimental T_g values were also fitted with respect to the values predicted by the Couchman–Karasz equation[18]: $\ln(T_{g,\text{blend}}/T_{g2}) = [w_1\Delta C_{p1} \times \ln(T_g/T_{g2})]/(w_1\Delta C_{p1} + w_2\Delta C_{p2})$. The T_g and ΔC_p values are available from the calorimetric measurements of the pure components. Again, fitting appears quite agreeable within the entire blend composition range. Once again, the T_g–composition relationships for either PVDF/PTA or PVDF/PPA blends are much better defined than those for other crystalline/crystalline PVDF/polyester blends, such as PVDF/PBA and PVDF/PBSu, previously reported in the literature.[3–7] The DSC traces showing clearer T_g signals and better defined T_g–composition relationships for the PVDF/PTA or PVDF/PPA blends are stronger evidence proving the miscibility. Nevertheless, generally for blends with marginal miscibility or T_g broadening, the T_g–composition relationship is expected to be below (i.e., negative deviation) what would be predicted by either a linear relationship or the Fox equation. The negative deviation (from the Fox T_g model or linearity) may indicate miscibility with either nonspecific (weak) interactions or some scales of microheterogeneous aggregation within a range of blend compositions (especially on the polyester-rich side).

Other thermal evidence, in addition to the blend T_g, such as the melting-point depression, is generally discussed to evaluate interactions. Figure 7 shows T_m of neat PVDF and PVDF/PPA blends (of several compositions) crystallized at a crystallization temperature (T_c) of 115–145°C. Note two features in the fig-

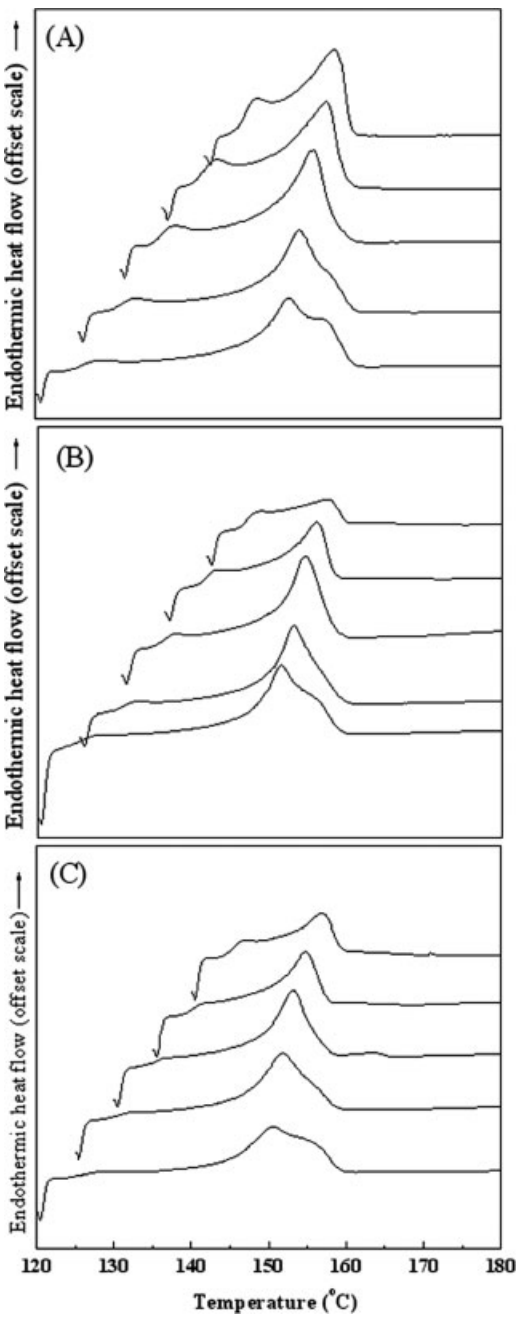

Figure 7 DSC traces (10°C/min) for (A) neat PVDF, (B) 70/30 PVDF/PPA, and (C) 50/50 PVDF/PPA isothermally crystallized at various temperatures for 8 h.

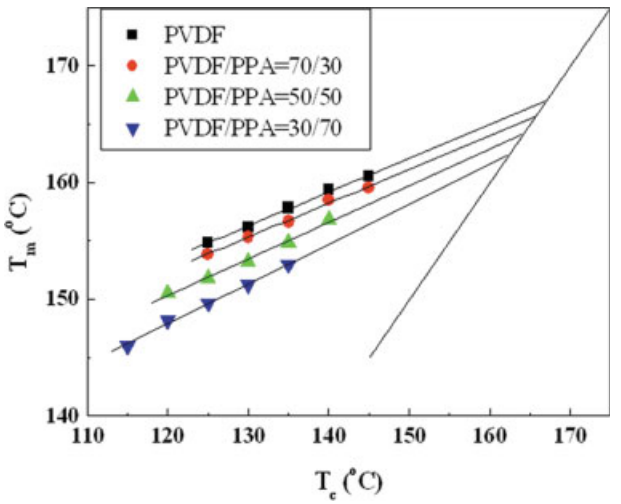

Figure 8 Hoffman–Weeks plots for neat PVDF and its blends isothermally crystallized at various temperatures for 8 h. [Color figure can be viewed in the online issue, which is available at www.interscience.wiley.com.]

ure. The polyester component, PPA, remains a liquid at these T_c's (115–145°C); thus, only the melting peak or peaks of PVDF are seen even if the blends of two crystalline polymers are at issue. Thus, the polyester constituent could be regarded as an amorphous species in the blend that acted as a diluent in lowering the melting of the PVDF crystallizing species. Thus, interactions between PVDF and a polyester, if any, could be estimated by the depression of T_m^0 of PVDF in the PVDF/polyester blends. Second, dual melting peaks are seen in either neat PVDF nor PVDF/polyester blends isothermally crystallized; however, extrapolation to T_m^0 can usually be based on the first peak (T_{m1}).

For high-molecular-weight polymers with folded-chain packing, T_m^0 values for a fully extended chain conformation are usually estimated by an extrapolation approach. T_m^0 values for PVDF in the blends were estimated by the following relationship proposed by Hoffman and Weeks:[19]

$$T_m = \eta T_c + (1 - \eta) T_m^0 \tag{1}$$

m is the slope of the Hoffman–Weeks plot.

Figure 8 shows representative plots according to the relationship for neat PVDF and PVDF/PPA blends (of three to four compositions). The extrapolation lines are reasonably linear for all blend compositions. The intercepts with the $T_m = T_c$ line yield the values of T_m^0 for blends. Because of the quite lengthy time of isothermal crystallization needed for each data point, it was not feasible to generate a large number of points for extrapolation; however, the limited data points do fall into a reasonably straight line with negligible data scattering.

Figure 9 shows a summary plot for the determination of interaction parameters for PVDF/PPA polyester blend systems, which is based on the following relationship[20]:

$$\left(\frac{1}{T_m^0(\text{blend})} - \frac{1}{T_m^0(\text{pure})}\right) = -\frac{RV_2}{\Delta H^\circ V_1}\left[\frac{\ln \phi_2}{m_2} + \left(\frac{1}{m_2} - \frac{1}{m_1}\right)\phi_1 + \chi_{12}\phi_1^2\right] \tag{2}$$

Equation (2) can be further rearranged to

$$-\left[\frac{\Delta H^0 V_1}{RV_2}\left(\frac{1}{T_m^0(\text{blend})} - \frac{1}{T_m^0(\text{pure})}\right) + \frac{\ln \phi_2}{m_2} + \left(\frac{1}{m_2} - \frac{1}{m_1}\right)\phi_1\right] = \chi_{12}\phi_1^2 \tag{3}$$

where R is the gas constant, ΔH^0 is the heat of fusion of the crystalline component, m is the degree of polymerization, ϕ is the volume fraction, V is the molar volume of the repeat unit and χ is the interaction parameter.

The physical constants needed for plotting were as follows: $\Delta H^0 = 5962$ J/mol, $V_1 = 185.7$ cm^3/mol, $V_2 = 36.4$ cm^3/mol,[11] $m_1 = 56$, and $m_2 = 1875$. Subscript 1 indicates the low-melting polyester, and subscript 2 indicates the higher melting PVDF. The densities for the two constituents were 1.78 cm^3/g for PVDF and 1.23 cm^3/g for PPA, which was assumed to be the same as that of PBA.[3] From analyses of the Flory–Huggins treatment[20] and plots of $\left(\frac{1}{T_m^0(\text{blend})} - \frac{1}{T_m^0(\text{pure})}\right)$ versus ϕ_1^2, a negative but quite small value of χ_{12} was obtained (-0.13) for the PVDF/PPA blend, which confirmed the miscibility and favorable, though not particularly strong, interactions between the constituents. A comparison with other blends shows that for the PVDF/PBA blend, $\chi = -0.19$[3,4]; for PVDF/PBSu, $\chi = -0.139$[5,6]; and for

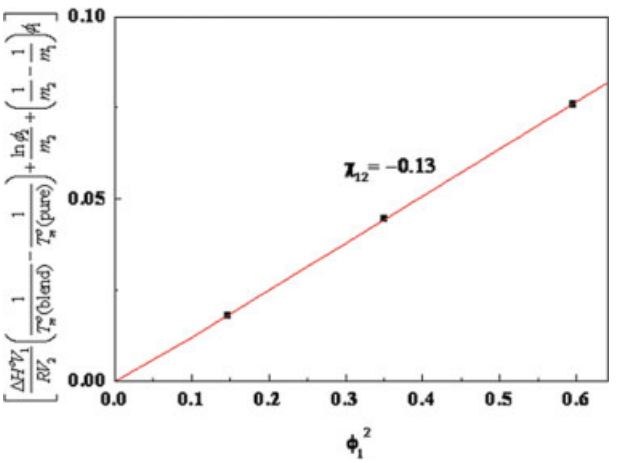

Figure 9 T_m^0 values of PVDF/PPA blends plotted according to the Flory–Huggins relationship with $\chi_{12} = -0.13$. [Color figure can be viewed in the online issue, which is available at www.interscience.wiley.com.]

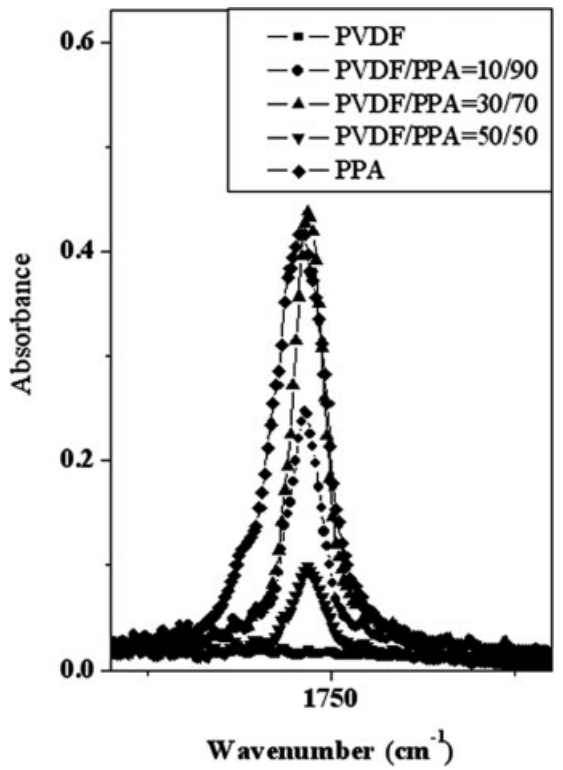

Figure 10 Carbonyl absorbance bands in FTIR spectra for PVDF/PPA blends of various compositions.

PVDF/PET, $\chi = -0.14$.[7] The fact of similar and small negative values shows that for most miscible blends of PVDF and polyesters, the interaction strength is generally quite weak. In a comparison of three blend systems (PVDF/PPA vs PVDF/PBA or PVDF/PBSu), the slight difference in the values of the interaction strength reflects the change in the structures of the polyester constituent in the PVDF/polyester blends.

FTIR characterization was used to verify the interaction strength between PVDF and polyester PPA. Figure 10 shows the carbonyl absorbance in FTIR spectra of neat PVDF, neat PPA, and three PVDF/PPA blends (10/90, 30/70, and 50/50). Other than changes in intensity with respect to the weight fraction of PPA in the blends, the wave number of the C=O absorbance remains almost stationary with respect to the blend composition, indicating no specific or strong interactions between C=O and $-CF_2$ groups. A similar result was found in FTIR spectra for PVDF/PTA blends. The IR results show that the interactions between PVDF and polyesters are quite weak and likely of a nonspecific nature.

Spherulite patterns in miscible and immiscible PVDF/polyester blends

Figure 11 shows POM graphs with enlarged spherulites (isothermally crystallized at 148°C) in neat PVDF in comparison with miscible PVDF/PPA blends of several representative compositions. Note that, for brevity, only a few representative blend compositions have been selected and are shown here for discussion. Apparently, ring bands can be seen in neat PVDF and miscible blends of PVDF with PPA ($CH_2/CO = 4.5$). Inset graphs on the right-hand side are corresponding patterns taken with nonpolarized light with aim of discerning amorphous phase domains. Neat PVDF (with neither crystalline nor amorphous diluents) is known to display fine ring bands, which can be discerned only with large enough magnification under POM. However, with increasing polyester contents in miscible PVDF/polyester blends, the ring-band pattern was found to be more distinct and coarser and could be easily detected with only medium magnifications. Furthermore, the interband spacing was found to be influenced by the polyester fraction in the PVDF/polyester blends. Patterns and ring spacing, however, differ significantly between neat PVDF and miscible blends. Note that there are fine and closely spaced ring bands in neat PVDF. In general, the concentric rings are coarser and spaced with a greater distance with increasing polyester contents in miscible PVDF/PTA or PVDF/PPA blends.

For miscible blends of PVDF and PTA ($CH_2/CO = 3.5$), the results are similar. Figure 12 shows POM graphs with ring-banded spherulites (isothermally crystallized at $T_c = 148$°C) in neat PVDF in comparison with miscible PVDF/PTA blends of several representative compositions. The band width in the miscible PVDF/PTA blends is influenced by the compositions. In comparison with the ultrafine rings in neat PVDF, ring bands are increasingly more apparent in blends. In addition, with increasing polyester contents in miscible blends, the band width becomes progressively larger. Note that in several crystalline/amorphous miscible blends, relationships between ring-band patterns and blend compositions have been discussed. However, the two miscible PVDF/polyesters in this study are crystalline/crystalline blends. Thus, the interpretation of ring-band patterns in crystalline/crystalline blends would have to be approached differently.

Literature-proven immiscible blends of PVDF/PEA and PVDF/PCL were also similarly examined with both POM and OM for comparison with the blends investigated in this study. However, in distinct contrast with the discussed miscible blends, for most immiscible blends, the ring bands become increasingly unclear, disrupted, or distorted with an increase in the polyester contents, with only some exception found in immiscible PVDF/PEA with less than 30 wt % PEA. From nonpolarizing OM (right column), the ring bands could not be distinguished. The spherulites in immiscible PVDF/polyester

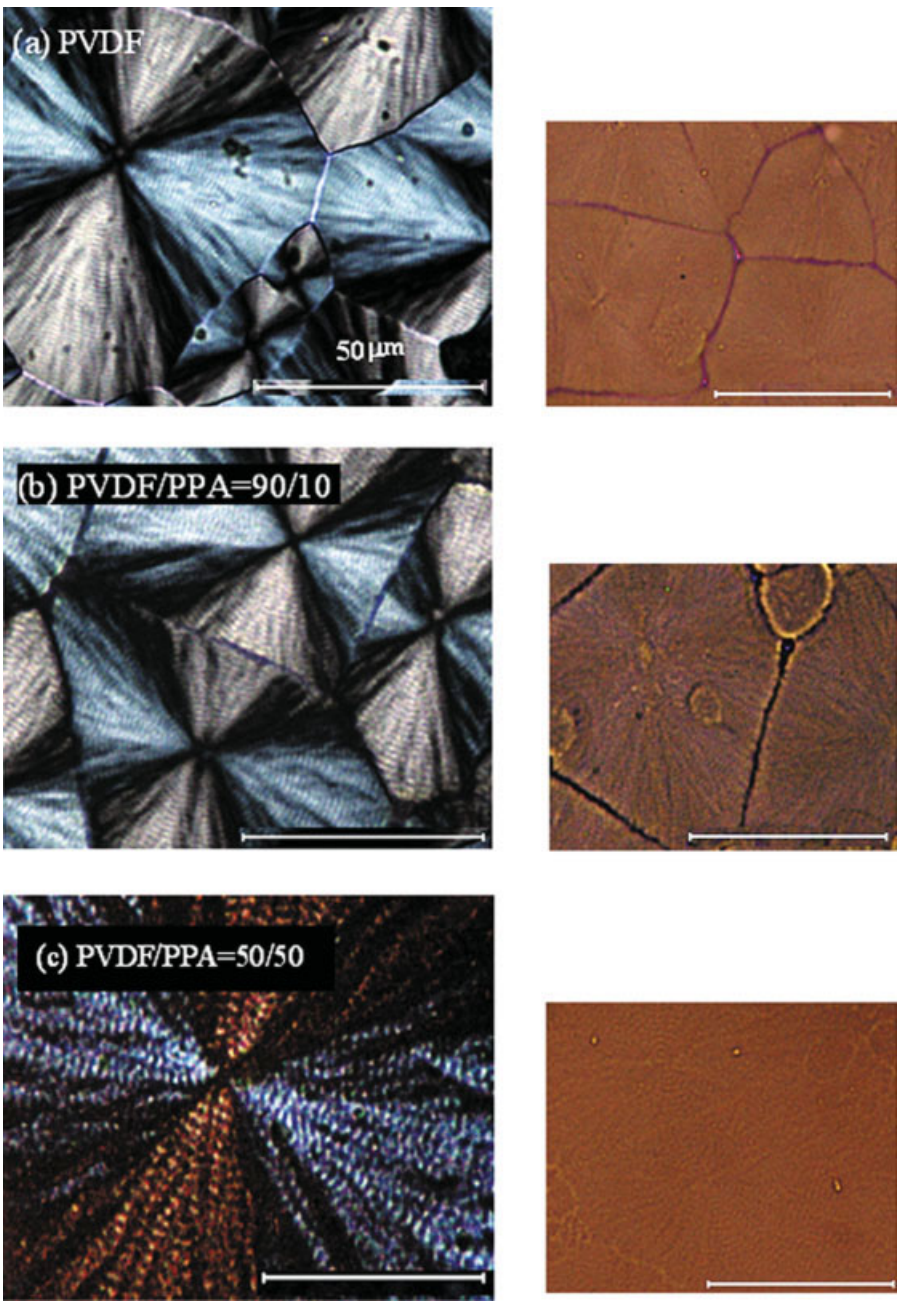

Figure 11 Ring-band spherulites (under POM) in (a) neat PVDF and in (b) 90/10 and (c) 50/50 PVDF/PPA blends. The insets on the right show micrographs with nonpolarized OM. [Color figure can be viewed in the online issue, which is available at www.interscience.wiley.com.]

blends are quite different from those in the miscible blends shown and discussed earlier. Figure 13 shows disrupted ring-band patterns (under POM) in immiscible PVDF/PEA blends of two compositions (70/30 and 50/50) and in immiscible PVDF/PCL blends of two compositions (70/30 and 50/50). The insets on the right-hand side show the OM micrographs of phase-separated domains taken with nonpolarized OM. Because of the ultrafine sizes of the phase-separated domains in immiscible PVDF/PEA blends, ring bands could still be detected in immiscible PVDF/PEA blends with low PEA contents (ca. $<$ 30 wt %). However, ring bands were significantly distorted and could not be discerned in the immiscible PVDF/PEA blends with PEA contents greater than 30 wt % in blends. Immiscible PVDF/PEA (70/30) is shown in this figure as an illustration. In comparison, the nonpolarized OM graphs [right-hand side insets to Fig. 13(c,d)] show that large, grainy phase-separation domains are present in PVDF/PCL blends. Consequently, the ring bands in immiscible PVDF/PCL are apparently distorted.

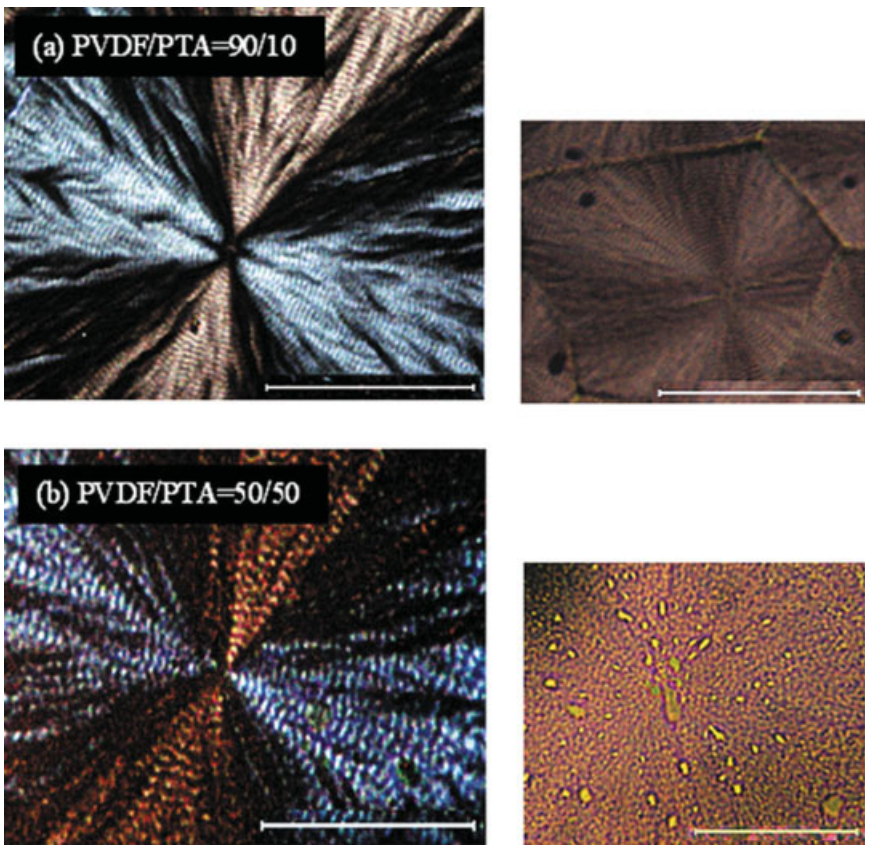

Figure 12 Ring-band spherulites (under POM) in miscible (a) 90/10 and (b) 50/50 PVDF/PTA blends. The insets on the right show micrographs with nonpolarized OM. [Color figure can be viewed in the online issue, which is available at www.interscience.wiley.com.]

The influence of miscibility or interactions on the ring bands in thin-film spherulites has also been reported in the literature. The subjects are mainly crystalline/amorphous miscible blends whose crystalline constituent shows ring bands in spherulites, and the interlamellar regions of spherulites have been proposed to be filled with more amorphous constituents. For example, effects of a miscible and amorphous diluent of poly(ether imide) on the ring-band morphology of poly(trimethylene terephthalate) have been investigated, and it has been concluded that rings become wider and coarser because of amorphous–crystalline species interactions in the blends.[21] However, such views on interpreting ring-band spacing in spherulites may be subjected to further debates if crystalline/crystalline blends (rather than crystalline/amorphous ones) are involved. Crystalline/crystalline blends and ring bands are relatively less studied. Note that PVDF/polyester blends are crystalline/crystalline systems, and interactions between PVDF and polyesters are quite weak, as demonstrated in this study; thus, interactions between amorphous and crystalline species may not apply to interpreting the widening or coarsening of the ring band in miscible PVDF/polyester blends.

Several crystalline/crystalline PVDF/polyester blends, such as PVDF/PBA,[4] PVDF/PBSu,[5] and PVDF/PHB,[8] can also exhibit changes in the band width or ring-band patterns, but quantitative relationships are yet to be established, and mechanisms need to be more properly interpreted for crystalline/crystalline blends. In general, in a comparison of neat PVDF with both miscible blend systems investigated, the spherulites in neat PVDF show a fine ring band superimposed with Maltese-cross birefringence patterns; in the two miscible blends (PVDF/PTA and PVDF/PPA blends), the spherulites also exhibit a concentric extinction ring band as well as a Maltese cross. An interesting feature is that ring spacing seems to be dependent on the fractions of the polyester contents in blends. Furthermore, Figure 14 shows ring-band spacing plotted as a function of the polyester weight fraction in PVDF/PTA and PVDF/PPA blends. The inter-ring spacing between the roughly concentric rings was accurately and carefully measured for neat PVDF and blends. For neat PVDF, the ring bands are fine, and inter-ring spacing was determined to be $\sim$ 1.0 μm; however, a roughly linear increase of inter-ring spacing (as well as scales of coarseness of rings) up to $\sim$ 2.5 μm was found for miscible blends (PVDF/PTA and PVDF/PPA with

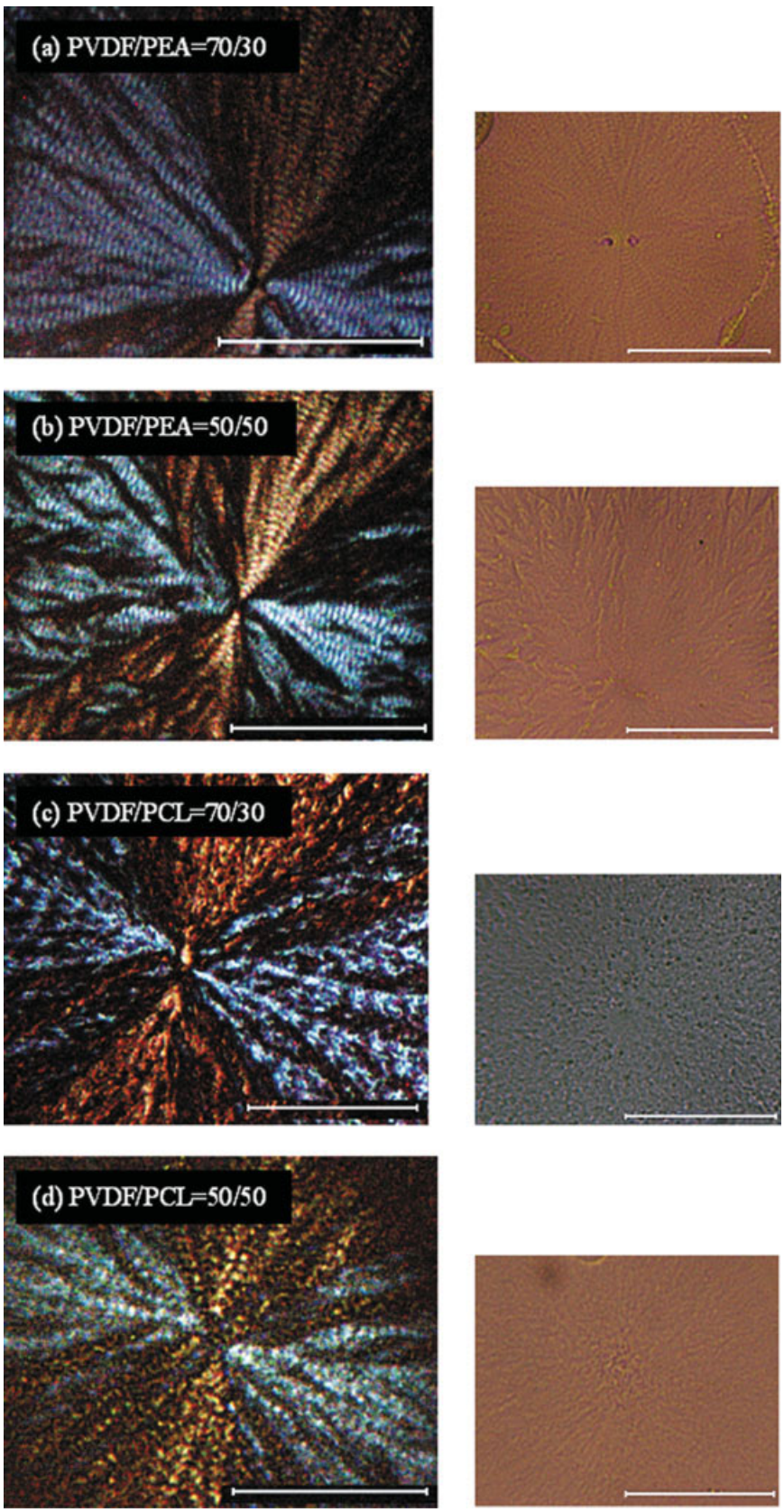

Figure 13 Disrupted ring-band patterns (under POM) in immiscible (a) 70/30 and (b) 50/50 PVDF/PEA blends and in immiscible (c) 70/30 and (d) 50/50 PVDF/PCL blends. The inset on the right show phase-separated domains with nonpolarized OM. [Color figure can be viewed in the online issue, which is available at www.interscience.wiley.com.]

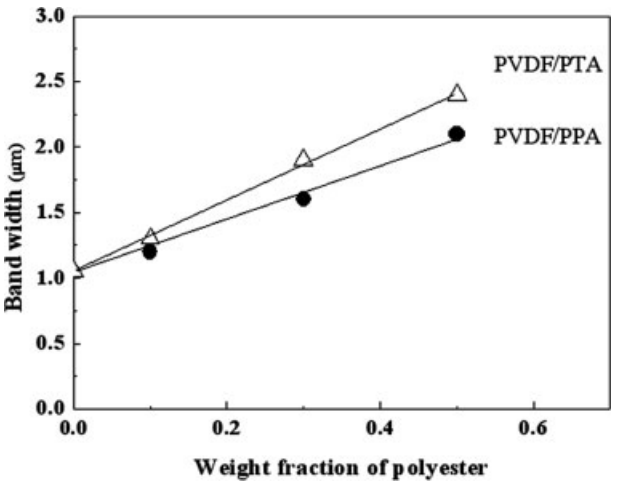

Figure 14 Ring-band spacing as a function of the polyester weight fraction in miscible PVDF/PTA and PVDF/PPA blends.

50 wt % polyester). For immiscible blends (e.g., a PVDF/PCL blend), ring patterns are either disrupted or nonexistent; thus, there are no data related to immiscible blends. Note that the increase in the ring-band spacing may also be accompanied by a corresponding increase in the coarseness of individual rings. The increase in coarseness and/or band spacing is generally taken as an indication and supportive evidence that miscibility does exist between the polyester and PVDF constituent in the blend.

CONCLUSIONS

This work further extends the range of polyester structures with which PVDF is miscible. In addition, relationships between ring-band patterns and miscibility in blends of PVDF with weakly crystallizing polyesters were investigated. PVDF was found to be miscible with PTA (with a CH_2/CO ratio of 3.5) and PPA (with a CH_2/CO ratio of 4.5), and this further extends the list of miscible blends involving PVDF and polyesters. Generally, blends of PVDF with polyesters exhibit borderline miscibility with weak interactions. The influence of phase miscibility on crystalline domains and ring-band patterns was investigated to assist the interpretation of the phase behavior in the amorphous domains. Favorable factors leading to miscibility in the blends are believed to originate from polar interactions between $—CF_2$ of PVDF and —C=O in polyesters. However, not all polyesters are miscible with PVDF, and the polyester structure tends to determine a range of most suitable electron negativity of —C=O for a favorable interaction with PVDF. FTIR spectroscopy has revealed that interactions between $—CF_2$ and —C=O group are weak, and the interaction parameters obtained with the DSC method for these blends have small, negative values.

The crystal domains in these miscible PVDF/polyester blends also exhibit interesting behavior. In general, the concentric rings are coarser and are spaced with a greater distance with increasing polyester contents in miscible PVDF/PTA or PVDF/PPA blends. An increase in coarseness and/or band spacing provides supportive evidence that miscibility does exist between the polyester and PVDF constituents in the blends. Ring-band behavior in the crystalline regions of the reported miscible blends was further used to substantiate the favorable, though relatively weak, interactions between the blend components.

References

1. Bernstein, R. E.; Wahrmund, D. C.; Barlow, J. W.; Paul, D. R. Polym Eng Sci 1978, 18, 1220.
2. Aubin, M.; Prud'homme, R. E. J Polym Sci Polym Phys Ed 1981, 19, 1245.
3. Penning, J. P.; St. John Manley, R. Macromolecules 1996, 29, 77.
4. Penning, J. P.; St. John Manley, R. Macromolecules 1996, 29, 84.
5. Lee, J. C.; Tazawa, H.; Ikehara, T.; Nishi, T. Polym J 1998, 30, 327.
6. Li, Y.; Kaito, A.; Horiuchi, S. Macromolecules 2004, 37, 2119.
7. Rahman, M. H.; Nandi, A. K. Macromol Chem Phys 2002, 203, 653.
8. Marand, H.; Collins, M. Polym Prepr 1990, 31, 552.
9. Edie, S. L.; Marand, H. Polym Prepr 1991, 32, 329.
10. Liu, J.; Qiu, Z.; Jungnickel, B. J. J Polym Sci Part B: Polym Phys 2005, 43, 287.
11. Nishi, T.; Wang, T. T. Macromolecules 1975, 8, 909.
12. Bernstein, R. E.; Cruz, C. A.; Paul, D. R.; Barlow, J. W. Macromolecules 1977, 10, 681.
13. Wahrmund, D. C.; Bernstein, R. E.; Barlow, J. W.; Paul, D. R. Polym Eng Sci 1978, 18, 677.
14. Kwei, T. K.; Patterson, G. D.; Wang, T. T. Macromolecules 1976, 9, 780.
15. Bernstein, R. E.; Paul, D. R.; Barlow, J. W. Polym Eng Sci 1978, 18, 683.
16. Okabe, Y.; Kyu, T.; Saito, H.; Inoue, T. Macromolecules 1998, 31, 5823.
17. Guo, Q. Eur Polym J 1996, 32, 1409.
18. Couchman, P. R.; Karaza, F. E. Macromolecules 1978, 11, 117.
19. Hoffman, J. D.; Weeks, J. J. J Res Natl Bur Stand A 1962, 66, 13.
20. Flory, P. J. Principles of Polymer Chemistry; Cornell University Press: Ithaca, NY, 1953.
21. Woo, E. M.; Wu, P. L. Colloid Polym Sci 2006, 284, 357.